Complete Reconstruction of the Wave Function of a Reacting Molecule by Four-Wave Mixing Spectroscopy

David Avisar and David J. Tannor

Department of Chemical Physics, Weizmann Institute of Science, Rehovot 76100, Israel

(Received 19 July 2010; published 29 April 2011)

Probing the real time dynamics of a reacting molecule remains one of the central challenges in chemistry. Here we show how the time-dependent wave function of an excited-state reacting molecule can be completely reconstructed from resonant coherent anti-Stokes Raman spectroscopy. The method assumes knowledge of the ground potential but not of any excited potential. The excited-state potential can in turn be constructed from the wave function. The formulation is general for polyatomics and applies to bound as well as dissociative excited potentials. We demonstrate the method on the Li_2 molecule.

DOI: 10.1103/PhysRevLett.106.170405 PACS numbers: 03.65.Wj, 31.50.Df, 78.47.nj, 82.53.−k

For several decades now, femtosecond pump-probe spectroscopies have been employed to study transition states of molecules reacting on excited potential surfaces [1–5]. Although these studies have shed a tremendous amount of light on excited-state dynamics, none of the methods in use provides complete information on the excited-state wave function. The need for an experimental method that will provide this information is compounded by the fact that theoretical *ab initio* calculations for excited states are difficult and of limited accuracy.

Several methods have been proposed for reconstructing excited-state wave functions from spectroscopic signals. Shapiro has suggested wave function imaging using the excited vibrational eigenstates as an expansion basis [6]. The coefficients are obtained from spectroscopic information and later used to reconstruct the excited potential, from which the basis is obtained. Cina has suggested a method of wave function reconstruction that assumes the excited-state potential is known [7]. There have also been various proposals for reconstructing excited-state potentials from spectroscopic data [8–12]. Experimental work has focused on wave packet interferometry of vibrational wave packets [13,14] as well as electronic Rydberg wave packets [15,16].

The approach we present here assumes knowledge of the ground-state potential but not of any excited potential. Our strategy is to express the molecular wave function $|\Psi(t)\rangle$ as a superposition of the vibrational eigenstates $\{|\psi_g\rangle\}$ of the ground-state Hamiltonian:

$$|\Psi(t)\rangle = \sum_g |\psi_g\rangle\langle\psi_g|\Psi(t)\rangle \equiv \sum_g C_g(t)|\psi_g\rangle. \quad (1)$$

Since the basis $\{|\psi_g\rangle\}$ is assumed known, the challenge is to find the time-dependent coefficients $C_g(t)$. Note that in principle the approach is general for polyatomics.

Consider a two-state molecular system within the Born-Oppenheimer approximation. The nuclear Hamiltonians H_g and H_e correspond, respectively, to the (known) ground and (unknown) excited potentials. For simplicity, we consider a δ-pulse excitation as well as a coordinate-independent electronic transition dipole μ (Condon approximation). By applying first-order time-dependent perturbation theory, the wave packet that we want to reconstruct is [17]

$$|\Psi(t)\rangle = -ie^{-iH_e t}\{-\mu\varepsilon_1\}|\psi_0\rangle \equiv i\mu\varepsilon_1|\psi(t)\rangle, \quad (2)$$

where the initial state $|\psi_0\rangle$ is the vibrational ground state of H_g with the eigenfrequency ω_0, ε_1 is the amplitude of the pulse, and t is the propagation time on the excited state. (Here and henceforth we take $\hbar = 1$.) Note that within a proportionality constant the excited-state wave packet $|\Psi(t)\rangle$ is equal to $|\psi(t)\rangle = e^{-iH_e t}|\psi_0\rangle$, the vibrational ground state of H_g propagated on H_e.

Substituting Eq. (2) into the middle expression in Eq. (1), we obtain $C_g(t) = i\mu\varepsilon_1 c_g(t)$, where

$$c_g(t) = \langle\psi_g|\psi(t)\rangle = \langle\psi_g|e^{-iH_e t}|\psi_0\rangle. \quad (3)$$

Hence, the central quantities required for reconstructing $|\Psi(t)\rangle$ are the overlaps $\langle\psi_g|\psi(t)\rangle$. These overlaps have a physical interpretation as the projections of $|\psi(t)\rangle$ onto the basis of ground vibrational eigenstates: As the wave packet moves on the excited-state potential, its *shadow* on the ground-state potential is completely recorded in these time-dependent projections. The rightmost expression in Eq. (3) indicates that $c_g(t)$ has the form of a time correlation function between $|\psi_0\rangle$ and $|\psi_g\rangle$. Such correlation functions appear in the time-dependent formulation of resonance Raman scattering [18]; however, the experimental resonance Raman scattering signal involves the absolute value squared of the half-Fourier transform of the correlation function, and hence the latter cannot be recovered from that signal.

Fully resonant coherent anti-Stokes Raman scattering (CARS) has been shown to be a powerful probe of ground and excited electronic states properties [19,20]. In this Letter, we show that the correlation functions $\{c_g(t)\}$ may

be completely recovered from femtosecond resonant CARS spectroscopy, allowing complete reconstruction of the excited-state wave packet. The formula for the CARS signal produced by a three-pulse sequence is $P^{(3)}(\tau) = \langle\psi^{(0)}(\tau)|\mu|\psi^{(3)}(\tau)\rangle + \text{c.c.}$ [21], where $\psi^{(3)}(\tau)$ is the third-order wave function and $\psi^{(0)}(\tau) = e^{-iH_g\tau}\psi_0$. Within the above assumptions, $P^{(3)}$ takes the form

$$P^{(3)}(\boldsymbol{\tau}) = \tilde{\varepsilon}\langle\psi_0|e^{-iH_e\tau_{43}}e^{-i\tilde{H}_g\tau_{32}}e^{-iH_e\tau_{21}}|\psi_0\rangle, \quad (4)$$

where $\tau_{ij} = \tau_i - \tau_j$ is the (positive) time delay between the centers of the ith and jth pulses and $\tau_{43} = \tau - \tau_3$ with τ being the time of signal measurement. We have denoted $\tilde{H}_g = H_g - \omega_0$, $\tilde{\varepsilon} = i^3\mu^4\varepsilon_1\varepsilon_2\varepsilon_3 e^{i\omega_0(\tau_{21}+\tau_{43})}$, with $\varepsilon_{1,2,3}$ as the first, second, and third pulse amplitudes, respectively, and $\boldsymbol{\tau} \equiv [\tau_{21}, \tau_{32}, \tau_{43}]$. In writing $P^{(3)}(\boldsymbol{\tau})$ as a complex quantity, we have assumed the signal is measured in a heterodyne fashion.

The physical interpretation of Eq. (4) is illustrated in Fig. 1: A first laser ("pump") pulse creates a wave packet that evolves on the excited potential for time τ_{21}. It is this wave packet that we wish to reconstruct. A second ("dump") pulse transfers part of this amplitude back to the ground state, where it evolves for time τ_{32}. Finally, a third pulse excites part of the second-order amplitude to the excited state, generating the third-order polarization that produces the CARS signal, measured after τ_{43}.

The wave packet $|\psi(t)\rangle$ [Eq. (2)] may be recognized in the rightmost factors in Eq. (4); the question is how to extract it. Since to reconstruct $|\Psi(t)\rangle$ we need only the correlation functions $\langle\psi_g|e^{-iH_e t}|\psi_0\rangle$, the problem reduces to extracting the latter from Eq. (4). Introducing a complete set of ground vibrational states, $\sum_g |\psi_g\rangle\langle\psi_g| = \hat{\mathbb{1}}$, into Eq. (4), we obtain the following suggestive formula for the signal:

$$P^{(3)}(\boldsymbol{\tau}) = \tilde{\varepsilon}\sum_g e^{-i\tilde{\omega}_g\tau_{32}}P_g^{(3)}(\tau_{43}, \tau_{21}), \quad (5)$$

where $P_g^{(3)}(\tau_{43}, \tau_{21}) = \langle\psi_0|e^{-iH_e\tau_{43}}|\psi_g\rangle\langle\psi_g|e^{-iH_e\tau_{21}}|\psi_0\rangle$ and $\tilde{\omega}_g = \omega_g - \omega_0$. Note that the desired correlation functions are closely related to the square roots of the $P_g^{(3)}$'s.

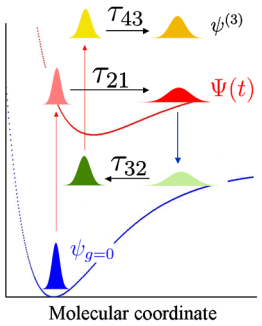

FIG. 1 (color online). The pump-dump-pump CARS scheme. $\Psi(t)$ is the desired wave function.

Thus, a general strategy for extracting the overlaps is clear: The signal $P^{(3)}(\boldsymbol{\tau})$ is Fourier transformed along τ_{32} to resolve the individual $P_g^{(3)}$'s. Then the square root of each $P_g^{(3)}$ is taken to obtain its corresponding $c_g(t)$. The $\{c_g(t)\}$ are then used to reconstruct $|\Psi(t)\rangle$. The details of the reconstruction are as follows.

1. Fourier transform $P^{(3)}(\boldsymbol{\tau})$ with respect to τ_{32}.—The transformation is designed to resolve $P^{(3)}(\boldsymbol{\tau})$ into individual ground-state components $\{P_g^{(3)}\}$ [22]. Using the Fourier convolution theorem we obtain a sinc type of spectrum with peaks at the frequencies $\omega = \tilde{\omega}_g$:

$$\tilde{P}^{(3)}(\tau_{43}, \omega, \tau_{21}) = \sum_{g=0}^{N} S(\omega, \tilde{\omega}_g)P_g^{(3)}(\tau_{43}, \tau_{21}), \quad (6)$$

where $S(\omega, \tilde{\omega}_g) = 2T\tilde{\varepsilon}e^{i(\omega-\tilde{\omega}_g)(\check{\tau}_{32}+T)}\,\mathrm{sinc}[(\omega - \tilde{\omega}_g)T]$, $2T = \hat{\tau}_{32} - \check{\tau}_{32}$, and $\check{\tau}_{32}$ ($\hat{\tau}_{32}$) is the minimal (maximal) value of τ_{32}. By fixing (τ_{43}, τ_{21}), Eq. (6) can be written as a matrix equation:

$$\tilde{\mathbf{P}}^{(3)} = \mathbf{S}\mathbf{P}_{\mathbf{g}}^{(3)}. \quad (7)$$

2. Invert Eq. (7) to obtain $P_g^{(3)}(\tau_{43}, \tau_{21})$.—To do this we need the matrix $\mathbf{S}$ to be square; we therefore choose the number of frequency elements ω equal to the number of $\tilde{\omega}_g$ elements and calculate $\mathbf{P}_{\mathbf{g}}^{(3)} = \mathbf{S}^{-1}\tilde{\mathbf{P}}^{(3)}$ [23].

3. Take the square root of $P_g^{(3)}$.—Assuming the functions $\{\psi_g(x)\}$ are real, we can rewrite $P_g^{(3)}$ as

$$P_g^{(3)}(\tau_{43}, \tau_{21}) = \langle\psi_g|e^{-iH_e\tau_{43}}|\psi_0\rangle\langle\psi_g|e^{-iH_e\tau_{21}}|\psi_0\rangle. \quad (8)$$

Taking the square root of the diagonal of $P_g^{(3)}(\tau_{43}, \tau_{21})$ (i.e., $\tau_{43} = \tau_{21} = t$), we recover the $\{c_g(t)\}$ up to a sign:

$$\sqrt{P_g^{(3)}(t)} = a_g\langle\psi_g|e^{-iH_e t}|\psi_0\rangle \equiv \langle\tilde{\psi}_g|e^{-iH_e t}|\psi_0\rangle, \quad (9)$$

where $a_g = \pm 1$ and the sign of $\tilde{\psi}_g(x)$ is as yet undetermined. By demanding continuity of the cross-correlation functions (and their derivatives), the coefficients a_g can be regarded as time-independent. Substituting Eq. (9) instead of $c_g(t)$ into the expression $C_g(t) = i\mu\varepsilon_1 c_g(t)$ and using the resulting $C_g(t)$ in Eq. (1) yields

$$|\tilde{\Psi}(t)\rangle = i\mu\varepsilon_1\sum_{g=0}^{N}|\psi_g\rangle\langle\tilde{\psi}_g|e^{-iH_e t}|\psi_0\rangle. \quad (10)$$

The different sign combinations of $\tilde{\psi}_g(x)$ generate 2^N possible superpositions [24]. Only one out of the 2^N $|\tilde{\Psi}(t)\rangle$ coincides with $|\Psi(t)\rangle$: the $|\tilde{\Psi}(t)\rangle$ for which the sign combination satisfies $\sum_g |\psi_g\rangle\langle\tilde{\psi}_g| = \hat{\mathbb{1}}$.

4. Discriminating $|\Psi(t)\rangle$ from the set $\{|\tilde{\Psi}(t)\rangle\}$.—The set of wave functions $\{|\tilde{\Psi}(t)\rangle\}$ are all consistent with the CARS signal at a specific value of $\tau_{43} = \tau_{21}$ [25]. However, only one $|\tilde{\Psi}(t)\rangle$ is consistent with the signal *derivatives*. To see

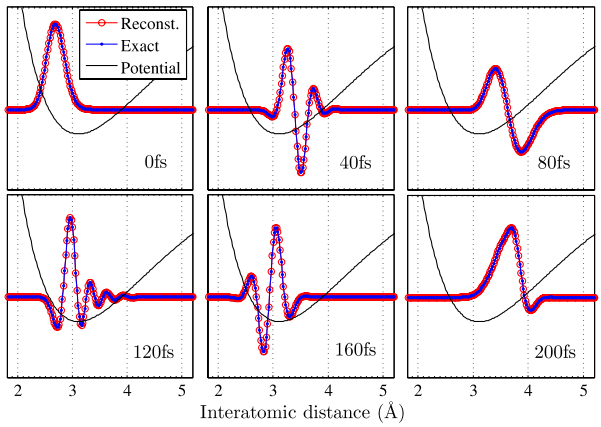

FIG. 2 (color online). Snapshots of the real part of the reconstructed (circles, red) vs the exact (dots, blue) wave function, at various times on the excited (A) potential (solid line) of Li_2.

this, consider the nth derivative of the experimental signal [Eq. (4)] with respect to τ_{21}:

$$\frac{\partial^n P^{(3)}(\boldsymbol{\tau})}{\partial \tau_{21}^n} = \varepsilon^\dagger \langle \Psi^*(\tau_{43}) | e^{-iH_g \tau_{32}} \tilde{H}_e^n | \Psi(\tau_{21}) \rangle = \varepsilon^\dagger \sum_{g,g'} e^{-i\omega_g \tau_{32}} C_g(\tau_{43}) C_{g'}(\tau_{21}) \tilde{H}^n_{e,gg'}, \quad (11)$$

where $\varepsilon^\dagger = (-i)^{n-1} \mu^2 \varepsilon_1^{-1} \varepsilon_2 \varepsilon_3 e^{i\omega_0 \tau_{41}}$, $\tau_{41} = \tau - \tau_1$, $\tilde{H}_e^n = (H_e - \omega_0)^n$, and $\tilde{H}^n_{e,gg'} = \langle \psi_g | \tilde{H}_e^n | \psi_{g'} \rangle$. Substituting $|\tilde{\Psi}(t)\rangle$ instead of $|\Psi(t)\rangle$ into Eq. (11) gives

$$\frac{\partial^n \tilde{P}^{(3)}(\boldsymbol{\tau})}{\partial \tau_{21}^n} = \varepsilon^\dagger \sum_{g,g'} e^{-i\omega_g \tau_{32}} a_g a_{g'} C_g(\tau_{43}) C_{g'}(\tau_{21}) \tilde{H}^n_{e,gg'}. \quad (12)$$

Accordingly, the $|\tilde{\Psi}(t)\rangle$ for which $\frac{\partial^n \tilde{P}^{(3)}(\boldsymbol{\tau})}{\partial \tau_{21}^n} = \frac{\partial^n P^{(3)}(\boldsymbol{\tau})}{\partial \tau_{21}^n}$ for all n is the reconstruction solution $|\Psi(t)\rangle$.

In practice, we proceed as follows. We invert the time-dependent Schrödinger equation to calculate a set of potentials from each $|\tilde{\Psi}(t)\rangle$:

$$\tilde{\tilde{V}}(x) = \frac{1}{\tilde{\Psi}(x,t)} \left[i \frac{\partial}{\partial t} + \frac{1}{2m} \frac{\partial^2}{\partial x^2} \right] \tilde{\Psi}(x,t), \quad (13)$$

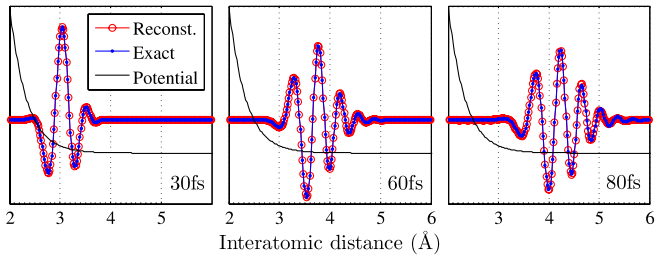

FIG. 3 (color online). Snapshots of the real part of the reconstructed (circles, red) vs the exact (dots, blue) wave function, at various times on the excited ($\tilde{A}$) potential (solid line) of d-Li_2.

where m is the system's reduced mass. One can show that the potentials calculated by the $|\tilde{\Psi}(t)\rangle$ that do not coincide with $|\Psi(t)\rangle$ are time-dependent [26]. Only the potential calculated with $|\tilde{\Psi}(t)\rangle = |\Psi(t)\rangle$ is time-independent and hence corresponds to the excited-state Hamiltonian H_e. Thus, in order to find the correct wave function we use the set of calculated potentials, as if they were time-independent, to propagate the corresponding $\{|\tilde{\Psi}(t)\rangle\}$ back to time zero. Of all the potentials, only the truly time-independent one will propagate the corresponding $|\tilde{\Psi}(t)\rangle$ correctly back to $|\psi_0\rangle$, and therefore this $|\tilde{\Psi}(t)\rangle$ is the correct wave function. Note that the above procedure requires knowing the signal as a function only of τ_{32} and $\tau_{21} = \tau_{43}$.

To test our reconstruction methodology, we simulated the CARS signal by calculating $P^{(3)}(\boldsymbol{\tau})$ for two systems. The first is the Li_2 molecule, with its ground (X) and first-excited (A) electronic states as Morse-type potentials $V(x) = D(1 - e^{-b(x-x_0)})^2 + T$. The second system, henceforth denoted d-Li_2, has the Li_2 ground state (X) but a dissociative excited potential of the form $V(x) = De^{-b(x-x_0)} + T$ (denoted $\tilde{A}$). The potential parameters are given in Ref. [26]. The wave packet propagations employed in simulating $P^{(3)}$ were performed by using the split-operator method [27] on a spatial grid of 256 points in the range of 2–12 a.u. with time spacing of 0.1 fs. We used $\mu = 2$ a.u. and $\varepsilon_{1,2,3} = 10^{-4}$ a.u. For Li_2, we inverted Eq. (7) for the first 25 peaks of $\tilde{P}^3(\omega)$, producing 25 $P_g^{(3)}$ functions; for d-Li_2, the procedure was performed for the first 40 peaks, producing 40 $P_g^{(3)}$ functions.

In Figs. 2 and 3, we present snapshots of the real part of the reconstructed wave function for Li_2 and d-Li_2, respectively. For Li_2 (d-Li_2) we superpose the first 25 (40) eigenfunctions $\psi_g(x)$ by using the $\{c_g(t)\}$ obtained by the CARS analysis and maintaining $\sum_g |\psi_g\rangle\langle\tilde{\psi}_g| = \hat{\mathbb{1}}$. The reconstructed wave functions are seen to be in excellent agreement with the exact ones, obtained by direct calculation of Eq. (2), for all propagation times.

Having determined the wave functions, we calculate the corresponding excited potential from Eq. (13) by using eight-point (three-point) central finite differencing for the time (spatial) derivatives; the time step used was 0.2 fs. Time steps of 0.5 fs gave very good results as well. Figures 4 and 5 compare the reconstructed vs the exact

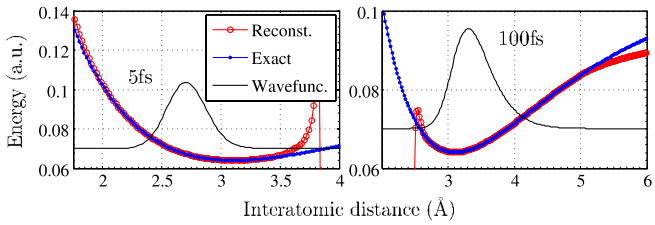

FIG. 4 (color online). The reconstructed (circles, red) vs the exact (dots, blue) A potential of Li_2.

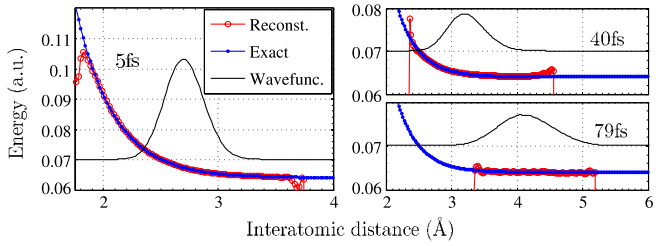

FIG. 5 (color online). The reconstructed (circles, red) vs the exact (dots, blue) $\tilde{A}$ potential of d-Li_2.

potentials. The wave function (absolute value) used to calculate the potential is shown by a black solid line.

In conclusion, we have presented a methodology for the complete reconstruction of the excited-state wave function of a reacting molecule by analyzing a multidimensional resonant CARS signal. The methodology is general for polyatomics and assumes that only the ground-state potential is known. The approach is very compelling since the desired excited-state wave function is explicitly contained in the formula for the CARS signal. Highly accurate reconstruction is obtained even far from the Franck-Condon region. In fact, in practice the method may be more accurate far from the Franck-Condon region, since the frequency shift between the pump and dump pulses will be more effective in discriminating unwanted processes that may contribute to the measured signal at $\mathbf{k} = \mathbf{k_1} - \mathbf{k_2} + \mathbf{k_3}$. We simplified matters by considering δ-function pulse excitations, a coordinate-independent transition dipole moment, and only one excited-state potential. In future work we will test the removal of all these assumptions.

We have shown that once the time-dependent wave function is found, the excited potential can be reconstructed with quite high accuracy. We are currently applying the method to polyatomics, where obtaining multidimensional potential surfaces from spectroscopic data has been one of the long-standing challenges of molecular spectroscopy. An important application of excited-state potential reconstruction will be the *ab initio* simulations of laser control of chemical bond breaking. Experimental laser control has been greatly hindered by the lack of detailed theoretical guidance, which in turn is due to the lack of accurate excited-state potentials. The present methodology could have a significant impact in this field by providing the necessary information about excited-state potentials.

This research was supported by the Minerva Foundation and by NSF Grant No. PHY05-51164, KITP preprint No. NSF-KITP-11-027. This research is made possible by the historic generosity of the Harold Perlman family.

[1] A. H. Zewail, Science **242**, 1645 (1988).
[2] J. C. Polanyi and A. H. Zewail, Acc. Chem. Res. **28**, 119 (1995).
[3] P. Kukura *et al.*, Science **310**, 1006 (2005).
[4] S. Takeuchi *et al.*, Science **322**, 1073 (2008).
[5] U. Banin and S. Ruhman, J. Chem. Phys. **99**, 9318 (1993).
[6] M. Shapiro, J. Chem. Phys. **103**, 1748 (1995); see also C. Leichtle *et al.*, Phys. Rev. Lett. **80**, 1418 (1998).
[7] J. A. Cina, J. Chem. Phys. **113**, 9488 (2000); Annu. Rev. Phys. Chem. **59**, 319 (2008). In the latter reference, the known excited state is not the one on which the wave function propagates.
[8] R. M. Roth, M. A. Ratner, and R. B. Gerber, Phys. Rev. Lett. **52**, 1288 (1984).
[9] R. B. Bernstein and A. H. Zewail, J. Chem. Phys. **90**, 829 (1989).
[10] T. Ho and H. Rabitz, J. Chem. Phys. **89**, 5614 (1988).
[11] R. Baer and R. Kosloff, J. Phys. Chem. **99**, 2534 (1995).
[12] M. Shapiro *et al.*, Phys. Chem. Chem. Phys. **12**, 15 760 (2010); X. Li and M. Shapiro, J. Chem. Phys. **134**, 094113 (2011).
[13] N. F. Scherer *et al.*, J. Chem. Phys. **95**, 1487 (1991).
[14] K. Ohmori *et al.*, Phys. Rev. Lett. **96**, 093002 (2006); K. Ohmori, Annu. Rev. Phys. Chem. **60**, 487 (2009).
[15] T. C. Weinacht, J. Ahn, and P. H. Bucksbaum, Phys. Rev. Lett. **80**, 5508 (1998).
[16] A. Monmayrant, B. Chatel, and B. Girard, Phys. Rev. Lett. **96**, 103002 (2006).
[17] D. J. Tannor, *Introduction to Quantum Mechanics: A Time-Dependent Perspective* (University Science, Sausalito, CA, 2007), Eq. (13.8).
[18] Soo-Y. Lee and E. J. Heller, J. Chem. Phys. **71**, 4777 (1979); E. J. Heller, R. L. Sundberg, and D. Tannor, J. Phys. Chem. **86**, 1822 (1982); A. B. Myers *et al.*, J. Chem. Phys. **77**, 3857 (1982); D. Imre *et al.*, J. Phys. Chem. **88**, 3956 (1984).
[19] P. L. Decola, J. R. Andrews, and R. M. Hochstrasser, J. Chem. Phys. **73**, 4695 (1980).
[20] N. A. Mathew *et al.*, J. Phys. Chem. A **114**, 817 (2010).
[21] J. Faeder *et al.*, J. Chem. Phys. **115**, 8440 (2001).
[22] Since τ_{32} is defined to be positive, we multiply Eq. (5), prior to the transformation, by the rectangular function that takes the value 1 for the τ_{32} domain and 0 elsewhere.
[23] For numerical accuracy, the inversion is implemented separately around each of the peaks $\tilde{\omega}_g$.
[24] Only 2^N are physically meaningful since we are free to set the sign of one of the g components.
[25] In fact, the set of wave functions given by Eq. (10) is consistent with the CARS signal for any pair (τ_{21}, τ_{43}).
[26] See supplemental material at http://link.aps.org/supplemental/10.1103/PhysRevLett.106.170405 for a proof of the time dependence of the potential $\tilde{V}$ [Eq. (13)] and a table containing the parameters used in the simulations.
[27] J. M. D. Feit, J. A. Fleck, and A. Steinger, J. Comput. Phys. **47**, 412 (1982).